Journal of Sound and Vibration (2000) **230**(2), 221–240
doi:10.1006/jsvi.1999.2617, available online at http://www.idealibrary.com on IDEAL®

A LOCK-FREE MATERIAL FINITE ELEMENT FOR NON-LINEAR OSCILLATIONS OF LAMINATED PLATES

GAJBIR SINGH AND G. VENKATESWARA RAO

Structural Engineering Group, Vikram Sarabhai Space Centre, Trivandrum - 695 022, *India*

(*Received* 13 *November* 1998, *and in final form* 1 *June* 1999)

The objective of the present paper is to propose an efficient, accurate and robust four-node shear flexible composite plate element with six degrees of freedom per node to investigate the non-linear oscillatory behavior of unsymmetrical laminated plates. The degrees of freedom considered are three displacement (u, v, w) along x-, y- and z-axis, two rotations (θ_x, θ_y) about y- and x-axis and twist θ_{xy}. The element employs coupled displacement field, which is derived using moment-shear equilibrium and in-plane equilibrium of composite strips along the x- and y-axis. The displacement field so derived not only depend on the element co-ordinates but are a function of extensional, bending–extensional, bending and transverse shear stiffness coefficients as well. A bi-cubic polynomial distribution with 16 generalized undetermined coefficients for the transverse displacement is assumed. The element stiffness and mass matrices are computed numerically by employing 3×3 Gauss Legendre product rules. The element is found to be free of shear locking and does not exhibit any spurious modes. The element is found to be free of shear locking and does not exhibit any spurious modes. In order to compute the non-linear frequencies, linear mode shape corresponding to fundamental frequency is assumed as the spatial distribution and non-linear finite element equations are reduced to a single non-linear second order ordinary differential equation. This equation is solved by employing direct numerical integration method. A series of numerical examples is solved to demonstrate the efficacy of the proposed material finite element.

1. INTRODUCTION

Fiber-reinforced composites, due to their high specific strength, high specific stiffness and anisotropic properties all of which can be tailored depending on the design requirement, are fast replacing the traditional metallic structures in the weight-sensitive aerospace and aircraft industries. These structures invariably experience severe dynamic environment during their service and thus the excited motions are likely to have large amplitudes. The large-amplitude analysis of composite structures is far more complex due to (i) anisotropy, (ii) material coupling and (iii) more pronounced transverse shear flexibility effects compared to their isotropic counterparts. These structures with complex boundary conditions, loading and shapes are not easily amenable to analytical solutions and hence one has to resort to numerical methods such as finite elements [1, 2]. A considerable amount of effort has gone into the development of simple plate bending elements based on the YNS theory [3] which is a consistent extension of the Mindlin's theory for homogeneous isotropic plates. The advantages of this approach are (i) it accounts for transverse shear deformation and (ii) it is possible to develop finite elements based on six engineering degrees of freedom (d.o.f.), namely three translations and three rotations [4]. However, the low-order elements, i.e., 3-node triangular, 4- and 8-node rectangular/quadrilateral elements lock and exhibit violent stress oscillations. To overcome this phenomenon, many techniques have been tried with varying degrees of success. The most prevalent technique to avoid shear locking for such elements is reduced or selective integration scheme [5–8]. The other notable successes are hybrid and mixed methods [9–12], the modified shear strain method [13, 14] and the field consistency [15–17] approach. In all these studies [5–14], shear stresses at nodes are unpredictable and need to be sampled at certain optimal points derived from the considerations based on the employed integration order [18]. The case of the shear locking phenomenon has been identified as the usage of same order polynomial approximations for the transverse displacement and section rotations. These independent polynomial approximations when substituted into the transverse shear strain expression lead to spurious constraints in the thin plate regime. The spurious constraints affect the bending energy severely and the element produces a highly stiff solution in an attempt to satisfy the Kirchhoff constraint. The techniques like reduced/selective integration do alleviate the problem of shear locking; however, in certain cases, zero-energy spurious modes get introduced. The severity of locking reduces considerably with the increase in the order of element. It is mainly because the inconsistency in transverse shear strain expression shifts to relatively less effective higher order terms than the linear terms in four-node elements. The 9- and 16-node Lagrangian elements for this reason are found to be relatively less affected and reasonably well behaved though computationally expensive [19, 20].

The subject of non-linear or large-amplitude vibrations of beams and plates has been of constant interest to many investigators since the first revelation of classical elliptical function solution of simply supported beams with immovable edges by Woinowsky-Krieger [21] and rectangular plates by Chu and Herrman [22]. Whitney and Leissa [23] formulated the governing equations for large-amplitude vibrations of heterogeneous anisotropic plates in the von Karman sense. Since then various approximate solution procedures and results have been reported by numerous investigators (refer to comprehensive surveys [24–27] and standard text books [28–30]). Sathyamoorty (25–27, 30] has reviewed more than a thousand papers on the topic of large-amplitude vibrations of plates. Singh *et al.* [31–33] proposed a direct numerical integration and modified Galerkin methods for accurate prediction of large-amplitude vibration behavior. They have also reported that the prevalent methods such as perturbation method and Galerkin method are inadequate for this purpose. The non-linear vibrations of beams and plates still continue to interest the researchers as reliable predictions of the large-amplitude motion are of great importance to avoid catastrophic failure [34]. As a consequence, new/different techniques are being attempted to study the phenomenon [33, 35, 36]. Further, the authors have found that in spite of the extensive literature available on the subject, suitable results for comparison are few. Most of the results available are in the graphical form and hence not suited for precise and accurate comparisons.

To date, the finite elements employed for the non-linear vibration analysis of beams and plates are based on independent polynomials of the same order for all the field variables. This type of elements with low order of interpolation approximation for field varibles exhibit sever shear locking in the case of thin plates if the associated element matrices are integrated exactly. Though quite a few approaches have been proposed over the years to eliminate the locking and associated problems caused by the independent and same order polynomial approximation for all field variables, a possible alternative displacement field has received little attention. The authors in their quest for an alternative displacement field, have realized the fact that in a flexural motion, the transverse displacement and section rotations are always coupled through transverse shear strain even for isotropic plates. In the case of an unsymmetrically laminated plate, the in-plane and out-of-plane responses are also coupled. This made the authors to believe that a properly derived, coupled displacement field would render an efficient, accurate, robust and lock-free plate element. This paper is a modest attempt towards this endeavor. The displacement field has been derived using equilibrium equations and is found to be a function of mechanical properties apart from the usual element geometry. To distinguish this class of elements from conventional ones, the authors felt it appropriate to classify them as material finite elements (MFE). In order to compute the non-linear frequencies, linear mode shape corresponding to fundamental frequency is assumed as the spatial distribution, and non-linear finite element equations are reduced to a single non-linear second order ordinary differential equation. The non-linear equation so obtained is typically Duffing's equation. However, in the case of unsymmetrically laminated plates, it contains an additional quadratic term. Direct numerical integration method is employed for the computation of non-linear frequencies. A series of numerical example is solved to demonstrate the efficacy of the proposed MFE element over a wide range of plate configurations.

2. GOVERNING EQUATIONS

Consider a rectangular plate composed of perfectly bonded layers of length "***a***", width "***b***" and total thickness "***h***" as shown in Figure 1. Each layer is made up of undirectional fibers and assumed to be a homogeneous orthotropic lamina. The orthotropic axes of symmetry in each lamina of arbitrary thickness and elastic properties are oriented at an arbitrary angle "α" to the x-axis of the plate. The components of displacement at a generic point in the plate are expressed in the form

$$U(x, y, z, \tau) = u(x, y, \tau) + z\theta_x(x, y, \tau),$$

$$V(x, y, z, \tau) = v(x, y, \tau) + z\theta_y(x, y, \tau),$$

$$W(x, y, z, \tau) = w(x, y, \tau). \tag{1}$$

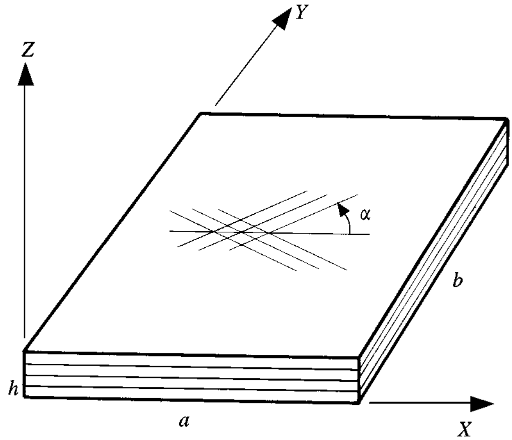

Figure 1. Geometry of a laminated plate.

In equation (1), u, v and w are displacements of the corresponding point on the middle plane, and θ_x and θ_y are rotations of the normal to middle plane about the y- and x-axis, respectively.

The non-linear membrane strains $(\varepsilon_x, \varepsilon_y, \gamma_{xy})$, curvatures $(\kappa_x, \kappa_y, \kappa_{xy})$ and transverse shear strains $(\gamma_{xz}, \gamma_{yz})$ are related to the displacements and rotations by the following equations:

$$\{\varepsilon\} = \begin{Bmatrix} \varepsilon_{xx} \\ \varepsilon_{yy} \\ \gamma_{xy} \end{Bmatrix} = \begin{Bmatrix} u_{,x} + \dfrac{1}{2} w_{,x}^2 \\ v_{,y} + \dfrac{1}{2} w_{,y}^2 \\ u_{,y} + v_{,x} + w_{,x} w_{,y} \end{Bmatrix}, \tag{2}$$

$$\{\kappa\} = \begin{Bmatrix} \kappa_{xx} \\ \kappa_{yy} \\ \kappa_{xy} \end{Bmatrix} = \begin{Bmatrix} \theta_{x,x} \\ \theta_{y,y} \\ \theta_{x,y} + \theta_{y,x} \end{Bmatrix}, \quad \{y\} = \begin{Bmatrix} \gamma_{xz} \\ \gamma_{yz} \end{Bmatrix} = \begin{Bmatrix} w_{,x} + \theta_x \\ w_{,y} + \theta_y \end{Bmatrix}, \tag{3,4}$$

where a comma followed by a subscript denotes differentiation with respect to the subscripted variable.

The membrane stress resultants (N_{xx}, N_{yy}, N_{xy}), stress couples (M_{xx}, M_{yy}, M_{xy}) and transverse shear forces (Q_{xz}, Q_{yz}) in a composite plate are related to the membrane strains, curvatures and transverse shear strains by the following constitutive relations:

$$\{N\} = [A]\{\varepsilon\} + [B]\{\kappa\}, \tag{5}$$

$$\{M\} = [B]\{\varepsilon\} + [D]\{\kappa\}, \tag{6}$$

$$\{Q\} = [S]\{\gamma\}. \tag{7}$$

In equations (5)–(7), A_{ij}, B_{ij} and D_{ij} $(i, j = 1, 2, 6)$ are the usual extensional, bending–extensional coupling and bending stiffness coefficients of the composite laminate; S_{lm} $(l, m = 4, 5)$ are the transverse shear stiffness coefficients of the laminate and include 5/6 as the shear correction factor.

The potential energy functional is given by

$$\Pi(u, v, w, \theta_x, \theta_y) = \frac{1}{2}\int_{\Omega} \{\{\varepsilon\}^{\mathrm{T}}[A]\{\varepsilon\} + \{\kappa\}^{\mathrm{T}}[B]\{\varepsilon\} + \{\varepsilon\}^{\mathrm{T}}[B]\{\kappa\} + \{\kappa\}^{\mathrm{T}}[D]\{\kappa\} + \{\gamma\}^{\mathrm{T}}[S]\{\gamma\} + R_r\dot{\theta}_x^2 + R_r\dot{\theta}_y^2 + R_t\dot{w}^2\}\,\mathrm{d}\Omega, \tag{8}$$

where R_r and R_t are the rotational and translational inertial and Ω is the domain of the plate.

3. MATERIAL FINITE ELEMENT FORMULATION (MFE)

The plate region Ω is decomposed into four-node rectangular finite elements having sub-domain Ω_e and interconnected at the four corners. Let the Cartesian co-ordinates of the nodes be (x_1, y_1), (x_2, y_2), (x_3, y_3) and (x_4, y_4) respectively. Among the five fundamental unknown u, v, w, θ_x and θ_y the transverse displacement field w is approximated by the complete bi-cubic as

$$w = c_1 + c_2x + c_3y + c_4x^2 + c_5xy + c_6y^2 + c_7x^3 + c_8x^2y + c_9xy^2 + c_{10}y^3 + c_{11}x^3y + c_{12}x^2y^2 + c_{13}xy^3 + c_{14}x^3y^2 + c_{15}c^2y^3 + c_{16}x^3y^3. \tag{9}$$

This field description was initially proposed by Bogner *et al.* [37] to develop a C^1 continuous rectangular plate bending element for the flexural response predictions of thin homogeneous isotropic plates. Singh *et al.* [31] employed the same field for the flexural analysis of moderately thick laminated composite plates. They employed a simple higher order theory involving only four field variables, i.e., u, v, w_b, w_s. The studies of references [31, 37] indicate that complete bi-cubic approximation for the transverse displacement w leads to a highly accurate and lock-free (in case of refere [31]) element. However, the accuracy is at the cost of a larger number of d.o.f. per node.

3.1. FIELD FOR IN-PLANE DISPLACEMENT u AND ROTATION θ_x

To derive the field for in-plane displacement u and section rotation θ_x, the equilibrium of a strip along the x-axis is considered. The equilibrium equations of the strip are obtained from the plate equilibrium equations by dropping terms involving derivatives with respect to y. These simplified equations are

$$A_{11}u_{,xx} + A_{16}v_{,xx} + B_{11}\theta_{x,xx} + B_{16}\theta_{y,xx} = 0, \tag{10}$$

$$A_{16}u_{,xx} + A_{66}v_{,xx} + B_{16}\theta_{x,xx} + B_{66}\theta_{y,xx} = 0, \tag{11}$$

$$B_{11}u_{,xx} + B_{16}v_{,xx} + D_{11}\theta_{x,xx} + D_{16}\theta_{y,xx} - A_{44}(w_{,x} + \theta_x) = 0, \tag{12}$$

$$B_{16}u_{,xx} + B_{66}v_{,xx} + D_{16}\theta_{x,xx} + D_{66}\theta_{y,xx} = 0, \tag{13}$$

$$A_{44}(w_{,xx} + \theta_{x,x}) = 0. \tag{14}$$

Making use of equations (10)–(14), $u_{,xx}$ and θ_x can be expressed as follows:

$$u_{,xx} = -\beta_1\theta_{x,xx} - \beta_3\theta_{y,xx}, \tag{15}$$

$$\theta_x = -w_{,x} + \alpha_1\theta_{x,xx} + \alpha_3\theta_{y,xx}, \tag{16}$$

where

$$\beta_1 = \frac{B_{11}A_{66} - A_{16}B_{16}}{A_{11}A_{66} - A_{12}^2}, \qquad \beta_3 = \frac{B_{16}A_{66} - A_{16}B_{66}}{A_{11}A_{66} - A_{12}^2},$$

$$\alpha_1 = \frac{(D_{11}A_{66} - B_{16}^2)(A_{11}A_{66} - A_{16}^2) - (B_{11}A_{66} - B_{16}A_{16})^2}{A_{44}A_{66}(A_{11}A_{66} - A_{16}^2)},$$

$$\alpha_3 = \frac{(D_{16}A_{66} - B_{16}B_{66})(A_{11}A_{66} - A_{16}^2) - (B_{11}A_{66} - B_{16}A_{16})(B_{16}A_{66} - B_{66}A_{16})}{A_{44}A_{66}(A_{11}A_{66} - A_{16}^2)},$$

Assuming that the transverse shear strains are predominantly constant, we substitute $\theta_x = -w_{,x}$ and $\theta_y = -w_{,y}$ on the right-hand side of equations (15) and (16) to obtain

$$u_{,xx} = \beta_1 w_{,xxx} + \beta_3 w_{,xxy} \tag{17}$$

or

$$u = \beta_1 w_{,x} + \beta_3 w_{,y} + c_{17} + c_{18}x + c_{19}y + c_{20}xy, \tag{18}$$

$$\theta_x = -w_{,x} - \alpha_1 w_{,xxx} - \alpha_3 w_{,xxy}. \tag{19}$$

Note: c_{17}–c_{20} are additional generalized undermined coefficients. These additional unknowns allow bilinear variation of in-plane displacement u in the absence of coefficients β_1 and β_3.

3.2. FIELD FOR IN-PLANE DISPLACEMENT v AND ROTATION θ_v

To derive the fields for in-plane displacement v and section rotation θ_y, equilibrium of a composite strip along the y direction is considered. The equilibrium equations are simplified by dropping terms involving derivatives with respect to x from the governing equations of a composite plate. Now, the procedure adopted in the derivation of the fields u and θ_x is adopted to arrive at the following field description for v and θ_y:

$$v = \beta_2 w_{,y} + \beta_4 w_{,x} + c_{21} + c_{22}x + c_{23}y + c_{24}xy, \tag{20}$$

$$\theta_y = -w_{,y} - \alpha_2 w_{,yyy} - \alpha_4 w_{,xyy}, \tag{21}$$

where

$$\beta_2 = \frac{B_{22}A_{66} - A_{26}B_{26}}{A_{22}A_{66} - A_{26}^2}, \qquad \beta_4 = \frac{B_{26}A_{66} - A_{26}B_{66}}{A_{22}A_{66} - A_{26}^2},$$

$$\alpha_2 = \frac{(D_{22}A_{66} - B_{26}^2)(A_{22}A_{66} - A_{26}^2) - (B_{22}A_{66} - B_{26}A_{26})^2}{A_{55}A_{66}(A_{22}A_{66} - A_{26}^2)},$$

$$\alpha_4 = \frac{(D_{26}A_{66} - B_{26}B_{66})(A_{22}A_{66} - A_{26}^2) - (B_{22}A_{66} - B_{26}A_{26})(B_{26}A_{66} - B_{66}A_{26})}{A_{55}A_{66}(A_{22}A_{66} - A_{26}^2)},$$

Note: c_{21}–c_{24} are additional generalized undermined coefficients. These additional unknowns allow bilinear variation of in-plane displacement v in the absence of coefficients β_2 and β_4.

It is interesting to note that a much desired higher order polynomial approximation for in-plane displacement fields (u, v) in the presence of bending-extension coupling is allowed by the fields derived herein. However, in the case of symmetrically laminated plates, the coefficients β's vanish and the field approximation for u and v reduces to bi-linear. The coefficients α's tend to vanish with the increase in side-to-thickness ratio and consistently satisfy the true Kirchhoff constraints of shearless bending, i.e., $\theta_x = -w_{,x}$ and $\theta_y = -w_{,y}$, in the extreme thin plate regime. Therefore, the element is expected to be free from shear locking.

To verify that the derived fields lead to a shear lock-free element, the transverse shear strains are expressed (using equations (9), (19) and (21)) as follows:

$$\gamma_{xz} = w_{,x} + \theta_x = -\{(6\alpha_1 c_7 + 2\alpha_3 c_8) + 6\alpha_3 c_{11} x + (6\alpha_1 c_{11} + 4\alpha_3 c_{12}) y + 12\alpha_3 c_{14} xy + (6\alpha_1 c_{14} + 6\alpha_3 c_{15}) y^2 + 18\alpha_3 c_{16} xy^2 + 6\alpha_1 c_{16} y^3\}, \quad (22)$$

$$\gamma_{yz} = w_{,y} = \theta_y = -\{(6\alpha_2 c_{10} + 2\alpha_4 c_9) + (6\alpha_2 c_{13} + 4\alpha_4 c_{12}) x + 6\alpha_4 c_{13} y + (6\alpha_4 c_{14} + 6\alpha_2 c_{15}) x^2 + 12\alpha_4 c_{15} xy + 18\alpha_4 c_{16} x^2 y + 6\alpha_2 c_{16} x^3\}. \quad (23)$$

It is evident from equations (22) and (23) that transverse shear strains will vanish as $\alpha_1 = \alpha_2 = \alpha_3 = \alpha_4 \Rightarrow 0$. As mentioned earlier, the magnitude of α's decreases continuously with the increase in side-to-thickness ratio of the plate and becomes practically zero for extremely thin plates. Hence, the vanishing of transverse shear strain does not impose any spurious constraints, whereas, in the case of the QUAD4 bi-linear element, the vanishing of transverse shear strains does lead to spurious constraints. The existence of these spurious constraints leading to shear locking in the case of elements involving independent field interpolations can be explained as follows.

Let the fields w, θ_x and θ_y be interpolated by the following bilinear independent polynomials:

$$w = r_1 + r_2 x + r_3 y + r_4 xy, \quad (24)$$

$$\theta_x = s_1 + s_2 x + s_3 y + s_4 xy, \quad (25)$$

$$\theta_y = t_1 + t_2 x + t_3 y + t_4 xy. \quad (26)$$

Using the field description (24)–(26), the transverse shear strains in a four-node bi-linear element can be written as

$$\gamma_{xz} = r_2 + s_1 + s_2 x + (r_4 + s_3) y + s_4 xy, \quad (27)$$

$$\gamma_{yz} = r_3 + t_1 + (r_4 + t_2) x + t_3 y + t_4 xy. \quad (28)$$

It is evident from equations (27) and (28) that vanishing of transverse shear strains $\gamma_{xz} \to 0$ and $\gamma_{yz} \to 0$ will impose the following spurious constraints:

$$s_2 = 0, \quad s_4 = 0, \quad t_3 = 0, \quad t_4 = 0, \tag{29–32}$$

The spurious constraints (29)–(32) are responsible for the shear locking behavior of four-node bilinear elements. The selective integration of shear energy, i.e., 1×2 for energy due to γ_{xz} and 2×1 for energy due to γ_{yz} would render the bi-linear element lock-free. If one expresses the shear strain expressions (27) and (28) in terms of Legendre polynomials, it will be evident that this selective integration is equivalent to dropping the terms involving s_2, s_4, t_3 and t_4. In the field consistency approach, proposed by Prathap and co-workers [15–17], terms involving s_2, s_4, t_3 and t_4 are dropped from the shear strain energy to obtain lock-free element. However, the presence of multiplying coefficient α's in shear strain expressions (22) and (23) makes all the constraints meaningful. Therefore, the proposed MFE does not require dropping of terms from the shear energy or selective integration of the same and still expected to yield consistently accurate results.

3.3. MATERIAL FINITE ELEMENT EQUATIONS

To solve for the 24 unknowns $(c_1, c_2, c_3, \ldots, c_{24})$, an additional d.o.f. θ_{xy} $(= \theta_{x,y} + \theta_{y,x})$ at each node is introduced apart from u, v, w, θ_x and θ_y. This additional twist d.o.f. is similar to the $w_{,xy}$ considered by Bogner *et al.* [37] and Singh *et al.* [31]. Substitution of displacement field equations (9) and (18)–(21) into potential function (8) and minimizing leads to the following finite element equations:

$$\{[k] + [n_1] + [n_2]\}\{\delta\} + [m]\{\ddot{\delta}\} = 0, \tag{33}$$

where $[k]$ is the linear element stiffness matrix of size 24×24, $[n_1]$, $[n_2]$ are the non-linear element stiffness matrix of size 24×24 depending on $\{\delta\}$ linearly and quadratically respectively, $[m]$ is the consistent mass matrix of size 24×24, and $\{\delta\}$ is the eigenvector of size 24×1.

The elemental matrices in the present study are integrated by employing the 3×3 Gauss quadarture formulae. These elemental equilibrium equations (33) are assembled using the standard procedure to obtain

$$\{[K] + [N_1] + [N_2]\}\{\delta\} + [M]\{\ddot{\delta}] = 0. \tag{34}$$

To compute the non-linear frequencies, the linear eigenvalue problem is solved as a first step. The eigenvector corresponding to the fundamental frequency is assumed as the spatial distribution and non-linear finite element equations are reduced to a single non-linear second order ordinary differential equation following the procedure given by Singh *et al.* [32]. The non-linear differential equation so obtained is of the following form:

$$\ddot{A} + \alpha A + \beta A^2 + \gamma A^3 = 0, \tag{35}$$

where α, β and γ are the coefficients of linear and non-linear stiffnesses and A denotes the maximum spatial deflection at any instant of time.

Equation (35) is solved by employing direct numerical integration method [32, 33] to compute the non-linear frequencies/periods as follows:

$$\frac{T}{2}=\frac{\pi}{\omega}=\int_0^{\pi/2}\frac{\mathrm{d}\theta}{\sqrt{\alpha[1+(2\beta/3\alpha)F_1(\theta)A_{max}+(\gamma/2\alpha)F_2(\theta)A_{max}^2]}}$$
$$+\int_0^{\pi/2}\frac{\mathrm{d}\theta}{\sqrt{\alpha[1+(2\beta/3\alpha)F_1(\theta)B_{max}+(\gamma/2\alpha)F_2(\theta)B_{max}^2]}} \qquad (36)$$

where $F_1(\theta)=(1+\sin\theta+\sin^2\theta)/(1+\sin\theta)$ and $F_2=1+\sin^2\theta$. A_{max} and B_{max} represent amplitudes of positive and negative deflection half-cycles. In the present analysis for a particular A_{max}, B_{max} is computed using the principle of energy conservation (for more details refer references [32, 33]). The integrands in equation (36) are computed numerically by employing a five-point Gauss quadrature formula.

4. NUMERICAL RESULTS

In this section, the performance of the proposed element (MFE) is assessed through a series of numerical examples involving effects of material coupling, transverse shear flexibility and boundary conditions. The present finite element (MFE) solutions, i.e., linear frequencies for various plate configurations, are compared with the corresponding QUAD4 element solutions. The bilinear quadrilateral element (QUAD4) based on selective integration is developed for the comparison purpose. Particular emphasis is laid on establishing the effects of anisotropy, shear deformation and edge restraints on the rate of convergence and accuracy with mesh refinement of the MFE elements. Throughout this section, numerical results are obtained by idealizing the whole plate. The non-linear frequencies for various plate configurations are computed using direct numerical integration method. The fundamental mode shape corresponding to 8×8 mesh discretization over the whole plate is used to computes the α, β and γ of equation (35).

The material properties and boundary conditions considered in this section are given in Tables 1 and 2.

4.1. INFINITESIMAL AMPLITUDE VIBRATION ANALYSIS

4.1.1. *Homogeneous isotropic plates*

The homogeneous isotropic plates with all edges simply supported (SSSS) or clamped (CCCC) are descretized with progressively refined meshes, i.e., 2×2, 4×4, $8\times 8,\ldots,32\times 32$ of MFE and QUAD4 elements. The variation of non-dimensional frequency parameter $\lambda_{\omega 0}$ corresponding to fundamental frequency ω_0 with mesh refinement for various side-to-thickness ratios (a/h = 5, 10, 100, 1000) is presented in Figures 2 and 3. It may be noted that the performance of the proposed MFE is

TABLE 1

Mechanical properties considered in the present study

Material	E_L/E_T	G_{LT}/E_T	G_{LZ}/E_T	G_{TZ}/E_T	υ_{LT}
M-I					0·3
M-II	25	0·5	0·5	0·2	0·25

TABLE 2

Boundary conditions considered in the present study

Boundary condition	Edge $x = 0, a$	Edge $y = 0, b$
Simple support (SSSS)	$u = v = w = \theta_y = 0$	$u = v = w = \theta_x = 0$
Clamped (CCCC)	$u = v = w = \theta_x = \theta_y = 0$	$u = v = w = \theta_x = \theta_y = 0$

far superior to the four-node (QUAD4). It is especially so when the side-to-thickness ratio is large or, in other words, when the plates are thin. In fact, in case of thin plates with all edges clamped, the authors found that even a 32×32 mesh of QUAD4 element over the whole plate does not yield converged frequencies. Thus, the convergence of traditional QUAD4 elements, based on independent interpolations is very slow. The frequencies obtained from the proposed elements are found to converge from the top in case of SSSS plates and from the bottom for plateswith all edges clamped. This behavior is typically that of a non-conforming element. It is because the present MFE employs coupled polynomial fields (refer to equations (19) and 21)), and thus the material coefficient α's and β's appearing in the displacement field are likely to influence its convergence characteristics. Though the convergence behavior of the proposed element is found to be function of boundary conditions, its rate of convergence is much faster than QUAD4.

4.1.2. *Four-layer symmetric cross-ply* $[0°/90°]s$ *plates*

The comparison of frequency parameter convergence characteristics of MFE with QUAD4 elements for square SSSS four-layered symmetric cross-ply plates is presented in Figure 4. As in the preceding study, the proposed MFE converges much faster, especially when plates are thin, than the conventional QUAD4 elements. The slower convergence of QUAD4 elements in the case of thin plates is an established problem (see reference 38) whose solution in the formal manner has been sought since long.

4.1.3. *Two-layer anti-symmetric cross- and angle-ply square plates*

The plate configuration considered so far did not involve material coupling ($\beta_i = 0$), and therefore in-plane and out-of-plane responses were uncoupled. The

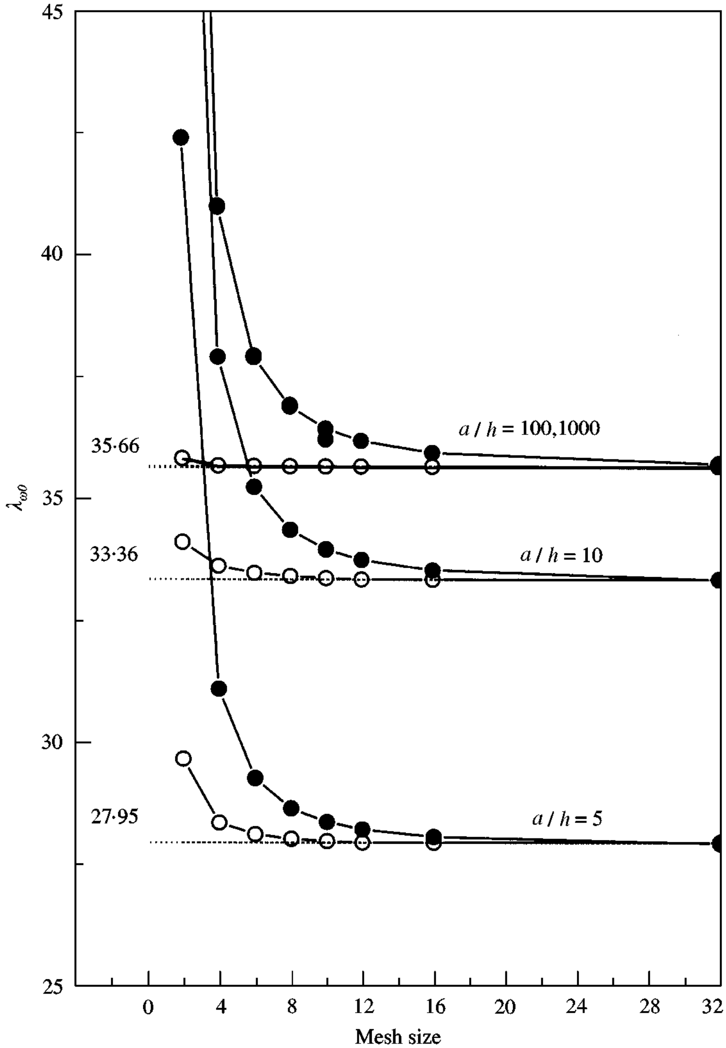

Figure 2. Comparison of frequency convergence characteristics of MFEM and QUAD4 for square simply-supported isotropic plates. —o— MFEM; —•— QUAD4; ..... converged.

response was governed by the transverse displacement and the two bending rotations. Thus, the only non-zero coupling coefficient in the displacement field were α's. However, in the case of antisymmetric cross- and angle-ply plates, the in-plane and out-of-plane responses are coupled. Therefore β's are non-zero. The non-zero β's allow higher order description of the in-plane displacement field and hence helps in accelerating the convergence. The comparison of convergence characteristics of frequency parameters of such plates obtained using MFE and QUAD4 is presented in Figures 5 and 6. It is obvious that MFE performs better than QUAD4. It may also be observed that the convergence in the case of two-layer angle-ply plates is from the top while for two-layer cross-ply plates, it is from the

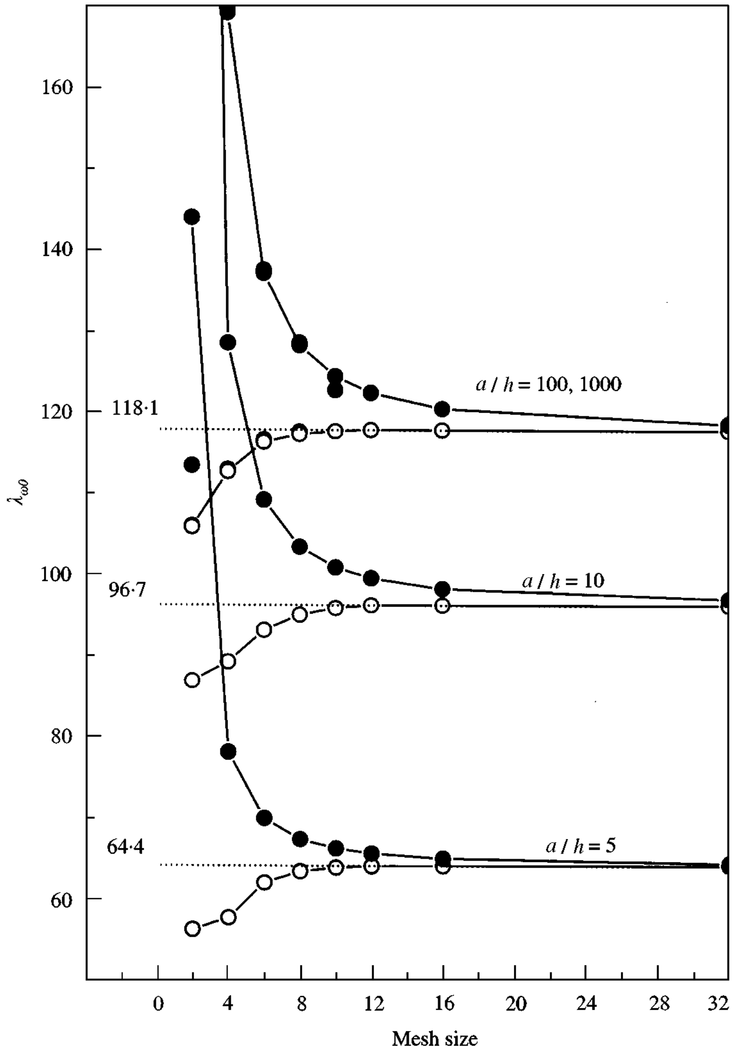

Figure 3. Comparison of frequency convergence characteristics of MFEM and QUAD4 for square isotropic plates with clamped edges. —o— MFEFM; —•— QUAD4; ..... converged.

bottom. This is because the coupled polynomial field employed in the two cases differ significantly owing to the values of α's and β's.

4.2. LARGE-AMPLITUDE VIBRATION ANALYSIS

The eigenvector corresponding to the fundamental frequency obtained using an 8×8 mesh over the whole plate is assumed as the spatial distribution herein and for the rest of the section to obtain the linear and non-linear stiffness coefficients of equation (35). Non-linear to linear frequency ratios (ω/ω_0) at different amplitudes are computed using *direct numerical integration method* for various plates configurations.

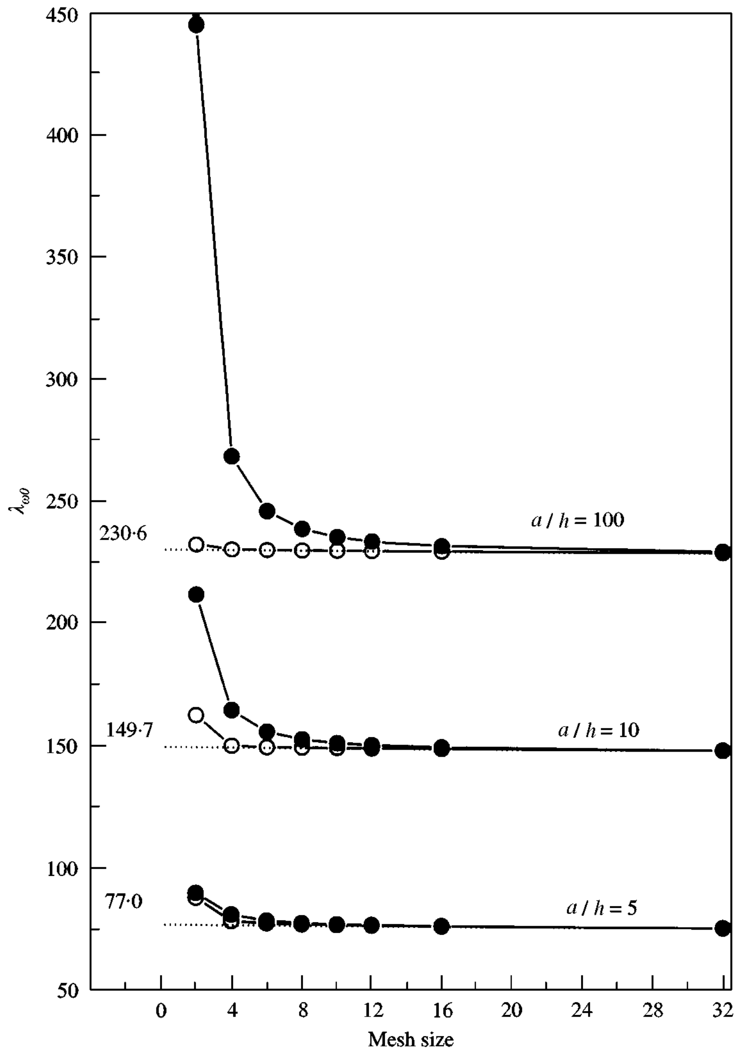

Figure 4. Comparison of frequency convergence characteristics of MFEM and QUAD4 for simply-supported cross-ply $[0°/90°]_s$ plates. —o— MFEFM; —•— QUAD4; ..... converged.

4.2.1. *Homogeneous isotropic square plates*

The variation of non-linear to linear frequency ratios (ω/ω_0) with amplitude-to-thickness ratio (A_{max}/h) for various side-to-thickness ratios is presented in Table 3. The edge conditions considered are (i) all edges are simply supported and (ii) all edges are clamped. The results indicate that the frequency increases with an increase in amplitude and decrease in side-to-thickness ratio. This is an expected trend because an increase in amplitude implies higher membrane tension.

4.2.2. *Four-layer symmetric cross-ply* $[0°/90°]_s$ *plates*

The variation of non-linear-to-linear frequency ratio ω/ω_0 with amplitude-to-thickness ratio for a four-layer symmetric cross-ply $[0°/90°]_s$ plate is presented in

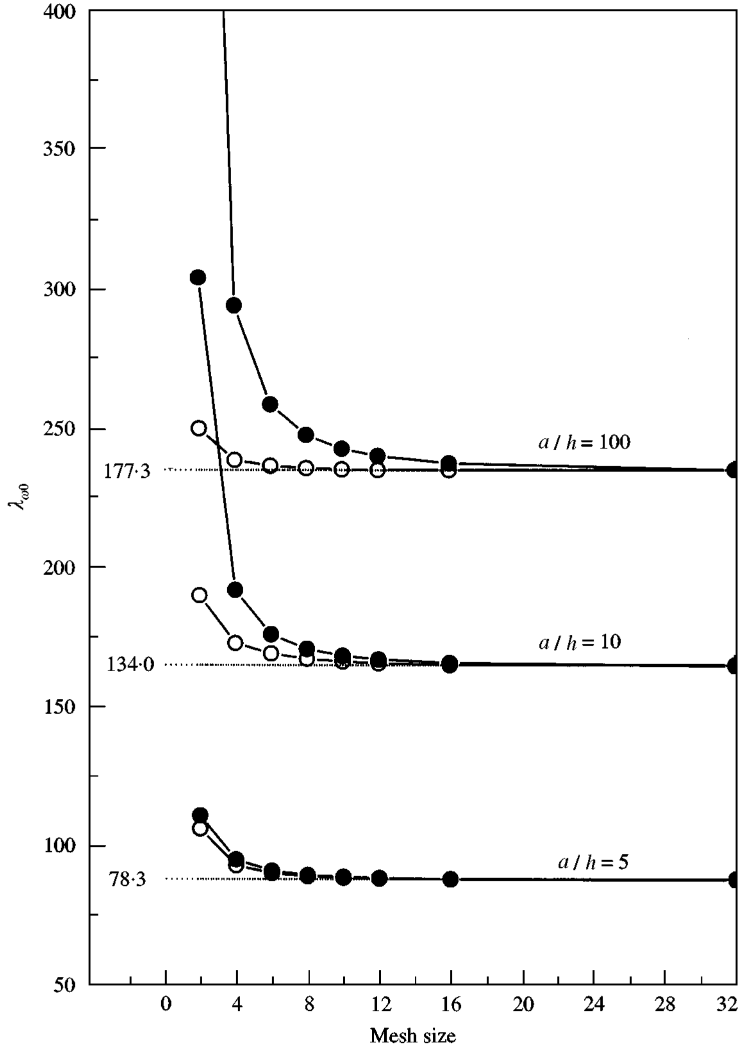

Figure 5. Comparison of frequency convergence characteristics of MFEM and QUAD4 for square simply-supported angle-ply [45°/ − 45°] plates. —o— MFEFM; —•— QUAD4; ..... converged.

Table 4. The mechanical properties for all the composite plates considered in this paper are of material M-II. The plates with all edges SSSS and side-to-thickness (a/h) 5, 10 and 100 are considered to investigate the effects of transverse shear flexibility on the non-linear frequencies. The study as expected indicates a non-linear frequency increase with an increase in amplitude, the increase being more for thick plates compared to thin plates. This indicates that the membrane stress generated in thick plates for the same amplitude ratio is higher than the corresponding one in thin plates.

4.2.3. *Two-layer cross- and angle-ply plates*

The non-linear stiffness coefficient β in equation (35) is zero for the preceding as well as the present study. For isotropic plates, it vanishes since bending–extension

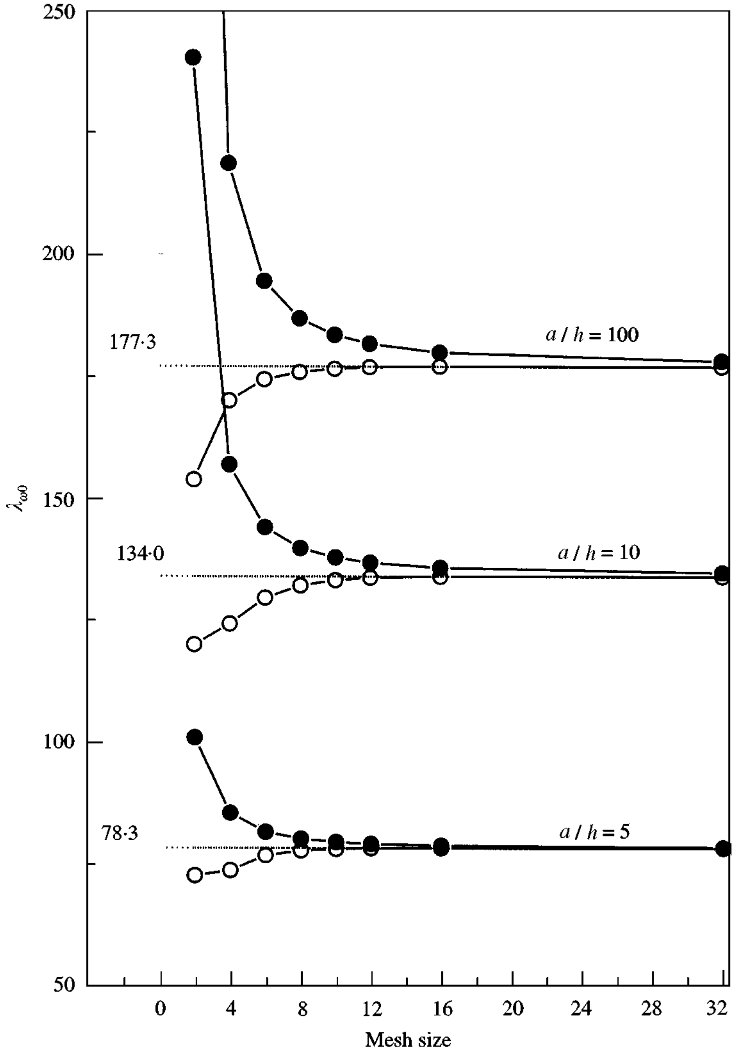

Figure 6. Comparison of frequency convergence characteristics of MFEM and QUAD4 for simply-supported cross-ply [0°/90°] plates. —o— MFEM; —•— QUAD4; ..... converged.

coupling coefficients B_{ij} are zero. However, in the particular case of a square antisymmetric cross-ply and even rectangular antisymmetric angle-ply plates, β is zero. Thus, the governing equation (35) is typically a Duffing's equation whose solution can be found either by the perturbation method or by the direct numerical integration method. It may be worth mentioning here that an exact elliptic integral solution of the Duffing's equations is also possible. The mechanical properties of material-II are considered in Tables 5 and 6. Table 4 indicates that two-layer cross-ply plates with simply supported edge conditions exhibit higher non-linearity compared to two-layer angle-ply plates. Similar results for rectangular ($a/b = 1{\cdot}2$) two-layer antisymmetric cross-ply and angle-ply plates with simply supported edges are presented in Table 6. It is found that for rectangular antisymmetric

TABLE 3

Variation of frequency ratio with amplitude ratio for square isotropic plates

$\pm A_{max}/h$	ω/ω_0					
	Simply supported (SSSS)			Clampled (CCCC)		
	$a/h = 100$	$a/h = 10$	$a/h = 5$	$a/h = 100$	$a/h = 10$	$a/h = 5$
0·2	1·020(1·0196)†	1·021	1·024	1·008(1·0086)‡	1·009	1·011
0·4	1·077	1·081	1·092	1·031	1·034	1·044
0·6	1·166(1·1642)	1·173	1·196	1·067(1·067)	1·074	1·096
0·8	1·279	1·291	1·328	1·117	1·128	1·164
1·0	1·411(1·4097)	1·427	1·478	1·177(1·176)	1·193	1·246
2·0	2·216	2·256	2·644	1·587	1·633	1·783

†Values in parentheses are taken from reference [39].
‡Values in parentheses are taken from reference [30].

TABLE 4

Variation of frequency ratio ω/ω_0 with amplitude for simply supported square four-layer cross-ply $[0°/90°]_s$ plates

$\pm A_{max}/h$	ω/ω_0		
	$a/h = 100$	$a/h = 10$	$a/h = 5$
0·2	1·032	1·047	1·086
0·4	1·120	1·174	1·309
0·6	1·253	1·358	1·609
0·8	1·416	1·579	1·952
1·0	1·601	1·823	2·318
2·0	2·681	3·195	4·289
$\lambda_{\omega 0}$	230·6	149·7	77·0

cross-ply plates, β in equation (35) does not vanish. Therefore such plates oscillate with different amplitudes in positive- and negative-deflection half-cycles, while antisymmetric angle-ply plates oscillte with the same amplitude in positive- and negative-deflection half-cycles.

The effects of CCCC on the variation of frequency ratio with amplitude are shown in Table 7. For this purpose, two-layer cross-ply and angle-ply square plates with side-to-thickness ratios 10 and 100 and made of material M-II are considered. The computation of coefficients α, β and γ reveals that the coefficient of quadratic term β vanishes for this case as well. On comparing the results of this table with the preceding study (Table 5), one finds that shear flexibility effects are more predominant in plates with clamped edges. The study shows that non-linearity effects are more pronounced in two-layered cross-ply plates than angle-ply plates.

TABLE 5

Variation of frequency ratio (ω/ω_0) with amplitude ratio for simply supported square two-layer cross-ply [0°/90°] and angle-ply [45°/ − 45°] plates

$\pm A_{max}/h$	ω/ω_0					
	[0°/90°]			[45°/ − 45°]		
	$a/h = 100$	$a/h = 10$	$a/h = 5$	$a/h = 100$	$a/h = 10$	$a/h = 5$
0·2	1·040	1·051(1·04)†	1·084	1·023	1·033	1·059
0·4	1·149	1·189(1·18)	1·300	1·089	1·120	1·212
0·6	1·310	1·387(1·38)	1·593	1·189	1·251	1·428
0·8	1·504	1·622(1·62)	1·928	1·316	1·413	1·683
1·0	1·722	1·880(1·88)	2·287	1·462	1·596	1·962

† Values in parentheses are deduced from reference [30].

TABLE 6

Variation of frequency ratio with amplitude ratio for rectangular ($a/b = 1{\cdot}2$) simply supported two-layer cross-ply [0°/90°] and angle-ply [45°/ − 45°] plates

A_{max}/h	[0°/90°]				[45°/ − 45°]			
	$a/h = 100$		$a/h = 10$		$a/h = 100$		$a/h = 10$	
	B_{max}/h	ω/ω_0	B_{max}/h	ω/ω_0	B_{max}/h	ω/ω_0	B_{max}/h	ω/ω_0
0·2	− 0·185	1·035	− 0·187	1·050	− 0·2	1·024	− 0·2	1·035
0·4	− 0·353	1·131	− 0·362	1·182	− 0·4	1·091	− 0·4	1·130
0·6	− 0·522	1·273	− 0·540	1·373	− 0·6	1·194	− 0·6	1·270
0·8	− 0·698	1·451	− 0·726	1·605	− 0·8	1·323	− 0·8	1·442
1·0	− 0·881	1·656	− 0·916	1·865	− 1·0	1·472	− 1·0	1·636
2·0	− 1·848	2·871	− 1·899	3·344	− 2·0	2·369	− 2·0	2·845

5. CONCLUSIONS

An accurate simple four-node shear flexible composite plate element based on coupled polynomial displacement field description is proposed in this paper for the investigation of non-linear oscillatory behavior of composite plates. The displacement field for the proposed MFE is derived from the equilibrium considerations, and hence it depends not only on the element co-ordinates, but on the material properties as well. The rate of convergence of QUAD4 elements is highly sensitive to the lay-up, side-to-thickness ratio and boundary conditions. The proposed MFE is practically insensitive to these parameters and continues to converge to accurate results with relatively coarse meshes. The element employs full Gaussian integration rules for computing the stiffness and mass matrices, and is

TABLE 7

Variation of frequency ratio (ω/ω_0) with amplitude ratio for clamped square two-layer cross-ply [0°/90°] and angle-ply [45°/ − 45°] plates

A_{max}/h	ω/ω_0			
	[0°/90°]		[45°/ − 45°]	
	$a/h = 100$	$a/h = 10$	$a/h = 100$	$a/h = 10$
0·2	1·023	1·033	1·017	1·028
0·4	1·087	1·122	1·067	1·099
0·6	1·186	1·253	1·144	1·208
0·8	1·311	1·416	1·244	1·344
1·0	1·455	1·600	1·360	1·500
2·0	2·325	2·676	2·086	2·434
$\lambda_{\omega 0}$	414·9	237·3	393·3	223·1

found to be free from shear locking and any spurious modes. The displacement fields of the MFE change with the lay-up sequence resulting in a convergence behavior similar to those of non-conforming elements. The direct numerical integration method employed herein does not assume temporal variation and yields highly accurate solutions. It is found that unsymmetrically laminated plates oscillate with different amplitude in positive- and negative-deflection half-cycles.

REFERENCES

1. O. C. ZIENKIEWICZ 1977 *The Finite Element Method*. London: McGraw-Hill, third edition.
2. K. J. BATHE 1990 *Finite Element Procedures in Engineering Analysis*. Englewood Cliffs, NJ: Prentice-Hall.
3. P. C. YANG, C. M. NORRIS and Y. STAVSKY 1966 *International Journal of Solids and Structures* **2**, 665–684. Elastic wave propagation in heterogeneous plates.
4. S. AHMED, B. M. IRONS and O. C. ZIENKIEWICZ 1970 *Computational Methods in Applied Mechanics and Engineering* **50**, 121–145. Analysis of thick and thin structures by curved finite elements.
5. O. C. ZIENKIEWICZ, R. L. TAYLOR and J. M. TOO 1971 *International Journal for Numerical Methods in Engineering* **3**, 275–290. Reduced integration techniques in general analysis of plates and shells.
6. S. F. PAWSEY and R. W. CLOUGH 1971 *International Journal for Numerical Methods in Engineering* **3**, 575–586. Improved numerical integration of thick shell finite element.
7. T. J. R. HUGHES, R. L. TAYLOR and W. KANOKNUKULCHAI 1977 *International Journal for Numerical Methods in Engineering* **11**, 1529–1543. A simple and efficient finite element for plate bending.
8. E. D. L. PUGH, E. HINTON and O. C. ZIENKIEWICZ 1978 *International Journal for Numerical Methods in Engineering* **12**, 1059–1079. A study of quadrilateral plate bending elements with reduced integration.
9. A. K. NOOR and C. M. ANDERSON 1977 *Computational Methods in Applied Mechanics and Engineering* **11**, 255–180. Mixed isoparametric finite element model of laminated composite shells.

10. S. W. Lee and T. H. Pian 1978 *American Institute of Aeronautics and Astronautics Journal* **16**, 29–34. Improvement of plate and shell finite elements by mixed formulations.
11. R. L. Spilker and N. I. Munir 1980 *International Journal for Numerical Methods in Engineering* **15**, 1239–1260. The hybrid stress model for thin plates.
12. R. Ayad, G. Dhatt and J. L. Batoz 1998 *International Journal for Numerical Methods in Engineering* **42**, 1149–1179. A new hybrid mixed variational approach for Reissner–Mindlin plates—the MiSP model.
13. T. J. R. Hughes and T. E. Tezduyar 1981 *Journal of Applied Mechanics* **48**, 587–596. Finite elements based upon Mindlin plate theory, with particular reference to the four-node bilinear isoparametric elements.
14. M. A. Crisfield 1984 *Computers and Structures* **18**, 833–852. A quadratic Mindlin element using shear constraints.
15. G. Prathap 1984 *Computers and Structures* **18**, 789–794. An optimally constrained 4-noded quadrilateral thin plate bending element.
16. G. Prathap 1985 *Computers and Structures* **21**, 995–999. A C^0 continuous 4-noded cylindrical shell element.
17. B. R. Somashekar, G. Prathap and C. R. Ramesh Babu 1987 *Computers and Structures* **25**, 345–353. A field consistent four-noded laminated anisotropic plate/shell element.
18. E. Hinton and J. S. Campbell 1974 *International Journal for Numerical Methods in Engineering* **8**, 461–480. Local and global smoothening of discontinuous finite element functions using a least square method.
19. H. C. Huang and E. Hinton 1984 *Engineering Computations* **1**, 369–379. A nine node lagrangian plate element with enhanced shear interpolation.
20. J. N. Reddy 1997 *Mechanics of Laminated Composite Plates—Theory and Analysis*. New York: CRC Press.
21. S. Woinowsky-Krieger 1950 *TRANS ASME*, *Journal of Applied Mechanics* **17**, 35–36. The effect of an axial force on the vibration of hinged bar.
22. H. N. Chu and G. Herrman 1956 *Journal of Applied Mechanics* **23**, 523–540. Influence of large amplitude on free vibrations of rectangular elastic plates.
23. J. M. Whitney and A. W. Leissa 1969 *Journal of Applied Mechanics* **36**, 261–266. Analysis of heterogeneous anisotropic plates.
24. M. Sathyamoorthy 1987 *Applied Mechanics Review* **40**, 1553–1561. Nonlinear vibration analysis of plates. A review and survey of current development.
25. M. Sathyamoorthy 1982 *Shock and Vibration Digest* **14**, 19–35. Nonlinear analysis of beams, Part I: a survey of recent advances.
26. M. Sathyamoorthy 1982 *Shock and Vibration Digest* **14**, 7–18. Nonlinear analysis of beams, Part II: finite element method.
27. M. Sathyamoorthy 1998 *Proceedings of* 8*th National Seminar on Aerospace Structures*, *IIT*, *Madras*, India, 9–10 *October* 1998, 198–213. Chennai, India: Allied Publishers Ltd., Recent research on large amplitude vibration of plates: a survey.
28. J. J. Stoker 1950 *Nonlinear Vibration in Mechanical and Electrical Systems*. New York: Inter Science Publishers.
29. A. H. Nayfeh and D. T. Mook 1979 *Nonlinear Oscillation*. New York: John Wiley.
30. M. Sathyamoorthy 1998 *Nonlinear Analysis of Structures*. New York: CRC Press.
31. G. Singh, G. Venkateswara Rao and N. G. R. Iyengar 1993 *Composites Engineering* **3**, 507–525. Large deflection behavior of shear deformable composite plates using a simple higher order theory.
32. G. Singh, G. Venkateswara Rao and N. G. R. Iyengar 1991 *American Institute of Aeronautics and Astronautics Journal* **29**, 1727–1735. Analysis of nonlinear vibrations of unsymmetrically laminated composite beams.
33. G. Singh and G. Venkateswara Rao 1998 *Acta Mechanica* **127**, 135–146. Nonlinear oscillations of thick asymmetric cross-ply beams.
34. S. Huang 1998 *Journal of Sound and Vibration* **214**, 873–884. Nonlinear vibrations of a hinged orthotropic circular plate with a concentric rigid mass.

35. M. I. QAISI 1997 *Journal of Sound and Vibration* **199**, 587–594. A power series solution for the nonlinear vibrations of beams.
36. A. Y. T. LELUNG and S. K. CHUI 1997 *Journal of Sound and Vibration* **204**, 239–247. Nonlinear vibration of the von Karman plate by IHB method.
37. F. K. BOGNER, R. L. FOX and L. A. SCHMIT 1996 *Presented at the Wright Patterson Air Force Base*, *Ohio Meeting on Matrix Methods in Structural Mechanics AFFDL-TR*-66-80, 397–443. The generation of inter-element compatible stiffness and mass matrices by the use of interpolation formulas.
38. H. V. LAKSHMINARAYANA and S. SRIDHARA MURTHY 1984 *International Journal for Numerical Methods in Engineering* **30**, 591–623. A shear-flexible triangular finite element model for laminated composite plates.
39. A. BHIMARADDI 1993 *Journal of Sound and Vibration* **162**, 457–470. Large amplitude vibrations of imperfect unsymmetric angle-ply laminated plates.